Strong magnetic field effect on over-the-barrier transport in Pb-p-$Hg_{1-x}Cd_xTe$ Schottky barriers

2013 Semicond. Sci. Technol. 28 035004

(http://iopscience.iop.org/0268-1242/28/3/035004)

Semicond. Sci. Technol. **28** (2013) 035004 (10pp) doi:10.1088/0268-1242/28/3/035004

Strong magnetic field effect on over-the-barrier transport in Pb-p-$Hg_{1-x}Cd_xTe$ Schottky barriers

V F Radantsev[1] **and V V Zavyalov**[2]

[1] Institute of Natural Sciences, Ural Federal University, Ekaterinburg 620000, Russia
[2] Department of Physics, Utah State University, 1600 Old Main Hill Logan, Utah 84322-4415, USA

E-mail: victor.radantsev@usu.ru

Received 24 September 2012, in final form 26 December 2012
Published 28 January 2013
Online at stacks.iop.org/SST/28/035004

Abstract

It is usually believed that the over-the-barrier current in Schottky barriers (SB) on p-type semiconductor is controlled by heavy holes. However, there is an additional potential barrier caused by an oxide layer inevitably existing at the interface in real SB. For typical parameters of the barrier, its tunnelling transparency for light holes can be higher by three orders of magnitude than that for heavy holes. Thus, one can expect that the current is mainly due to the contribution of light holes. To clarify this problem, the investigation of carrier transport in a magnetic field is used as a key experiment in this work. The notable magnetic field effect for heavy holes in Pb-p-$Hg_{1-x}Cd_xTe$ SB investigated is expected only at magnetic fields $B > 10$ T. However, experimentally more than twofold decrease in the saturation current is observed even at $B \sim 0.5$ T. The studies performed on $Hg_{1-x}Cd_xTe$ with different Kane's gap, at numerous magnetic field orientation and at various temperatures show that the magnitude of the magnetic field effect is uniquely determined by the ratio of the light hole cyclotron energy to the thermal energy, $\theta = \hbar\omega_{clh}/kT$. However, the experimental dependences of the saturation current do not follow the exponential decay ($\propto \exp(-\theta/2)$) predicted by a simple theory. A more sophisticated theoretical model is needed for data interpretation.

1. Introduction

To date, the alloy semiconductor $Hg_{1-x}Cd_xTe$ owing to its unique properties remains the leading variable gap semiconductor for infrared photoconductive and photovoltaic detectors including imaging sensor system of third generation (focal plane arrays, two-colour detectors, hyperspectral arrays, etc) [1, 2]. One of the challenging structures for building photosensitive cell is the Schottky diode which, as the majority carrier device, has a faster response compared to photodiodes. In the case of narrow gap $Hg_{1-x}Cd_xTe$ ($x < 0.4$), the Schottky barriers exhibit rectifying properties only in the structures grown on p-type material. In addition to the over-the-barrier current (dominated carrier transport mechanism in wide-gap semiconductor devices), the barrier structures fabricated on the narrow gap $Hg_{1-x}Cd_xTe$ semiconductor exhibit significant contribution of tunnelling currents, which limit diode performance. The mechanisms of tunnelling in Pb-p-$Hg_{1-x}Cd_xTe$ SB were studied in our previous works [3, 4]. Due to a small effective mass the light holes dominate in tunnelling current through the SB grown on p-$Hg_{1-x}Cd_xTe$. As a result, the strong magnetic field effect on tunnelling was observed in these structures [4].

As for the over-the-barrier carrier transport, it is conventional to assume that heavy holes give the dominant contribution to this current component in Schottky barriers (SB) fabricated on p-type semiconductors. The over-the-barrier current in ideal SB associated with the jth carrier type is described by the expression [5]

$$I_j = I_{0j}\left[\exp\left(\frac{eV_b}{kT}\right) - 1\right], \tag{1}$$

where e is the electronic charge, T is the absolute temperature, k is the Boltzmann constant, V_b is the voltage drop across the

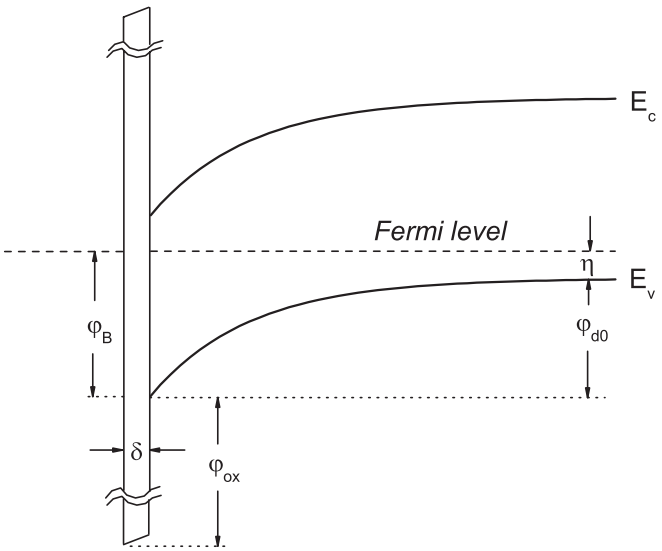

Figure 1. The schematic energy diagram of a Schottky barrier on a p-semiconductor with an interface dielectric layer at a zero bias.

barrier (the voltage for forward bias is chosen as positive) and I_{0j} is the saturation current expressed by

$$I_{0j} = Sep_j\overline{v}_j \exp\left(\frac{-\varphi_{d0}}{kT}\right) = SA_j^*T^2 \exp\left(\frac{-\varphi_B}{kT}\right) \qquad (2a)$$

or

$$I_{0j} = Sep_j v_{dj} \exp\left(\frac{-\varphi_{d0}}{kT}\right) = SA_j^*T^{3/2}\left(\frac{4\pi m(\varphi_{d0} - eV_b)}{k\varepsilon\varepsilon_0}\right)^{1/2} \exp\left(\frac{-\varphi_B}{kT}\right) \qquad (2b)$$

within the framework of the diode (thermionic emission) or diffusion theory, respectively. In equations (2*a*) and (2*b*), S is SB surface area, p_j is the concentration of the jth carrier type, $\overline{v}_j = \sqrt{kT/2\pi m_j^*}$ is an average thermal velocity, m_j^* is the effective mass, $A_j^* = ek^2m_j^*/2\pi^2\hbar^3$ is the effective Richardson constant, $\hbar$ is Planck constant, $\varphi_{d0} = \varphi_B - \eta$ is a diffusion potential (band bending) at zero bias (see figure 1), φ_B is the Schottky barrier height, η is an energy difference between the bulk Fermi level and valance band edge, $v_{dj} = \mu_j E_m$ is a drift velocity, μ_j is the mobility, E_m is a maximum electric field in the space-charge region and ε and ε_0 are the permittivities of the semiconductor and free space, respectively.

The 'classical' argument for neglecting the contribution of the light holes in the thermionic current in SB is based on the fact that the ratio between the heavy holes (hh) and light hole (lh) currents

$$\frac{I_{\rm hh}}{I_{\rm lh}} = \frac{p_{\rm hh}\overline{v}_{\rm hh}}{p_{\rm lh}\overline{v}_{\rm lh}} = \frac{m_{\rm hh}^*}{m_{\rm lh}^*}\left[1 + \frac{15}{4}\frac{kT}{E_g}\left(1 + \frac{kT}{E_g}\right)\right]^{-1} \qquad (3)$$

is proportional to the ratio of carrier effective masses. The factor in brackets in equation (3), where E_g is the Kane's energy gap, arises because of the non-parabolicity of light hole band. In the case of narrow gap semiconductor $Hg_{1-x}Cd_xTe$, the light holes must contribute according to this assumption less than 5% to the total current even for $x = 0.3$. However, the above argumentation is true only for an ideal SB but is not justified for the real SB. When the metal layer is deposited on the semiconductor surface a native oxide is typically formed on the interface during SB formation. Thus, a thin dielectric layer separating the metal and semiconductor (with thickness typically around 1 nm) is inevitably present in real Schottky diodes. In recent years, SBs with an intentionally grown thin dielectric layer (metal–insulator–semiconductor Schottky diodes) were a subject of increasing interest [6, 7]. In such structures, an interfacial layer serves to stabilize the metal–semiconductor interface and minimize the interface-trapped charges. In the presence of the additional potential barrier caused by the dielectric layer, the current density through the SB is reduced by the value of the quantum-mechanical penetration coefficient, P. In the case of a rectangular potential barrier, the P value is given in WBK approximation by

$$P_j = \exp\left(-\frac{2\sqrt{2}}{\hbar}\delta\sqrt{m_{tj}^*\varphi_{\rm ox}}\right), \qquad (4)$$

where $m_{tj}^* \approx (1/m_0 + 1/m_j^*)^{-1}$ is the tunnelling (reduced) mass [8] for the jth carrier type, m_0 is the rest mass of the electron and δ and $\varphi_{\rm ox}$ are the thickness and barrier height of the interfacial insulator layer, respectively. For typical thickness $\delta = 1$ nm and reasonable value of the barrier height $\varphi_{\rm ox} = 1$ eV, equation (4) gives $P_{\rm hh} \sim 7 \times 10^{-4}$ and $P_{\rm lh} \sim 0.36$ for heavy ($m_{\rm thh}^* \sim 0.5m_0$) and light ($m_{t\rm lh}^* \sim 0.01m_0$) holes, respectively. Therefore, an oxide layer is relatively transparent for light carriers (electrons and light holes) and practically impenetrable for heavy holes. If the presence of a potential barrier from the interfacial insulator is taken into account, the ratio between the heavy- and light-holes current is then given by

$$\frac{I_{\rm hh}}{I_{\rm lh}} = \frac{p_{\rm hh}\overline{v}_{\rm hh}P_{\rm hh}}{p_{\rm lh}\overline{v}_{\rm lh}P_{\rm lh}} \approx \frac{m_{\rm hh}^*}{m_{\rm lh}^*}\left[1 + \frac{15}{4}\frac{kT}{E_g}\left(1 + \frac{kT}{E_g}\right)\right]^{-1} \times \exp\left[-\frac{2\sqrt{2}}{\hbar}\delta\varphi_{\rm ox}\sqrt{m_{\rm hh}^*}\left(1 - \sqrt{m_{\rm lh}^*/m_{\rm hh}^*}\right)\right]. \qquad (5)$$

For the δ, $\varphi_{\rm ox}$, $m_{\rm lh}^*$ and $m_{\rm hh}^*$ values chosen above the estimated ratio of $I_{\rm hh}/I_{\rm lh}$ is 0.07 at $T = 100$ K. Thus, for real SBs as compared to ideal SBs one can assume an inverse relation between the currents arising from the light and heavy holes $I_{\rm lh} \gg I_{\rm hh}$. Generally speaking, there are some indirect arguments supporting this assumption. An analysis of the literature reveals extremely small experimental values of the Richardson constant A^* (by factor $\sim 10^2$) in SB Pb, Au, Ti, Al, Cr-p-HgCdTe [3, 13, 14] in comparison with its theoretical value making the typical assumption that heavy holes dominant current transport in SBs on the base of p-semiconductors. However, in real SB the large discrepancy between the experimentally observed A^* and its theoretical value can be attributed to the inferior diode quality. Even for SB with low-ideality factors, the experimental values of the Richardson constant can vary several orders of magnitude.

In order to examine unambiguously whether the light carriers dominate in over-the-barrier transport, one can use the magnetic field known to modify the current–voltage (I–V) characteristics. Two quantities in the expression for current (1) can be affected by the magnetic field: (i) Schottky barrier height φ_B due to an increase in the effective energy gap

Table 1. Sample proprieties (alloy composition x, energy gap E_g and doping level $N_A - N_D$) and basic Schottky barrier characteristics (temperature corresponding to the transition from a regime of tunnelling to a regime of thermionic emission T_0, Schottky barrier height φ_B, ideality factor β, effective Richardson constant A_0^* and barrier height lowering due to the image force $\Delta\varphi_{\text{im}}$). The A_0^* and φ_B values correspond to the low temperature segment of the Richardson plot (see section 5).

sample	x	E_g [a] (meV)	$N_A - N_D$ (cm^{-3})	T_0 (K)	φ_B [a] (meV)	β	A_0^* $\text{A·m}^{-2}\text{K}^{-2}$	$\Delta\varphi_{\text{im}}$ [b] (meV)
PK2	0.221	94	4.0×10^{15}	80	75	1.15	150	5.0
C37	0.290	210	1.5×10^{15}	110	160	1.05	60	5.3
C36	0.289	208	6.0×10^{15}	100	165	1.05	65	8.2

[a] At $T = 0$ K.
[b] At zero bias and $T = 140$ K.

$E_g(B) = E_g(0) + \Delta E_g(B)$, where $\Delta E_g(B)$ is of the order of cyclotron energy $\hbar\omega_c = \hbar eB/m^*$; (ii) the mobility $\mu(B) = \mu(0)(1+\mu(0)^2B^2)^{-1}$ (in the case of diffusion transport only). It is evident from equations (2*a*) and (2*b*) that the values of the effect are determined by the parameters $\theta = \hbar\omega_c/kT$ and $\mu(0)B$ in first and second cases, respectively. Due to a small effective mass and high mobility of light holes, the magnetic field should suppress the light hole component of the current while the heavy-hole component is hardly affected. Therefore, application of a magnetic field enables a precise experimental separation between these two components.

The influence of a magnetic field on the carrier transport in Schottky barriers was investigated in work [4] at low temperatures, when the tunnelling current dominates. However, we have not found any studies of magnetic field effects on the over-the-barrier transport in SB. Most likely, this is due to extremely small magnitude of the effect expected in Schottky barriers on the base of both wide- and narrow-gap semiconductors, because in the latter case the rectifying contacts are implemented only on p-type materials.

The results of the first study of the over-the-barrier carrier transport in Pb-p-$Hg_{1-x}Cd_xTe$ Schottky barriers in a magnetic field at high temperatures are reported in this paper. The carrier effective mass is a critical parameter defining the origin and magnitude of the magnetic field effect. To investigate magnetic field-effect dependences on the light hole effective mass, the samples with the several alloy composition x were investigated. Note that in narrow gap semiconductors $Hg_{1-x}Cd_xTe$ the electron and light hole effective masses decrease dramatically with a decreasing composition parameter x.

2. Experimental details

The semiconductor substrates, used in this work were p-type vacancy-doped bulk single crystals. Polished plates were etched in a 5% solution of Br_2 in methanol for 5–10 s with subsequent deposition of a thick insulating film to provide mounting areas for the SB electrodes. Directly before the evaporation of the metal, the structures were subjected to a brief (1–2 s) etching in a solution of the same composition as before. Omission of one of these operations resulted in a drastic deterioration of the Schottky barrier characteristics. Typical SB surface areas were $S = 10^{-4} - 2 \times 10^{-3}$ cm^2. Measurements were carried out on the best-quality structures with the lowest value of the ideality factor and the smallest leakage current. The Schottky diodes with such proprieties and a high reproducibility of the characteristics were obtained only in the case of Pb-p-HgCdTe structures. The high quality of SB with Pb metal contact is evidently due to high values of the tetrahedral radius and saturation vapour pressure of Pb as compared to other metals. These properties should minimize the structural damage during evaporation and diffusion of the metal into HgCdTe because its surface is known to be easily damaged due to a weakness of the chemical bonds.

The alloy composition, energy gap and doping level of the samples investigated in this study are listed in table 1. The heavy-hole mobilities are $\mu_{\text{hh}} = 450, 400$ and 420 $\text{cm}^2\ \text{V}^{-1}\ \text{s}^{-1}$ for samples PK2, C37 and C36, respectively. The values of $N_A - N_D \approx p_{\text{hh}}$ and μ_{hh} were determined from the Hall measurements at 77 K. The sample temperature was monitored by a copper–constantan thermocouple and temperature controller with an accuracy of better than 0.2 K.

3. Current–voltage characteristics in magnetic field

The typical current–voltage characteristics for sample C37 at high temperatures $T > T_0$ at which the over-the-barrier transport dominates (the typical T_0 values are listed in table 1) are presented in figure 2 with magnetic field as a parameter. In a non-ideal SB, the I–V characteristic deviates from the simple expression (1). The leakages, barrier height dependence on the voltage, recombination in the space-charge region, tunnelling across the potential barrier and carrier trapping by the interface states modify the nature of the carrier transport in real SB. In addition, part of the applied voltage drops across a series resistance R_s of the bulk material. An ideality factor, $\beta > 1$, is commonly used to model phenomenologically the effect of all the nonidealities ($\beta = 1$ for pure thermionic emission) [5, 9]

$$I = I_s \exp\left[\frac{e\,(V - IR_s)}{\beta kT}\right]\left[1 - \exp\left[\frac{e\,(V - IR_s)}{kT}\right]\right]. \quad (6)$$

As shown in figure 2, the forward branch of I–V characteristics in SB studied is well accounted for by equation (6) with and without the magnetic field. The ideality factor estimated from the linear part of the $\ln\left\{I/\left[1 - \exp\left(eV_b/kT\right)\right]\right\} - V$ curves at $T > T_0$ does not depend appreciably on the temperature and does not change with magnetic field. At $T < T_0$, the tunnel current prevails and the value $\beta kT = E_0$ is independent of the temperature leading to $\beta \propto 1/T$. The magnetic field effect on the forward branch of the I–V characteristics is simply a

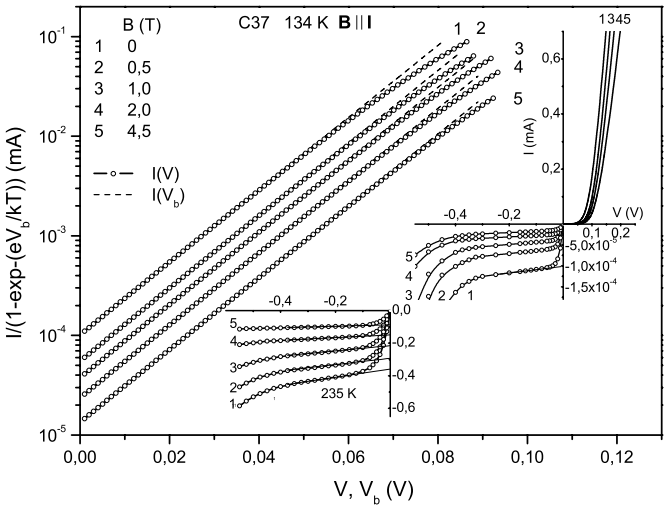

Figure 2. Logarithmic plot of $I/[1-\exp(eV/kT)]$ versus forward bias V and voltage drop across the barrier $V_b = V - IR_s$ (R_s is the series resistance) at various magnetic fields for sample C37. The experimental I–V characteristics are shown in the insets.

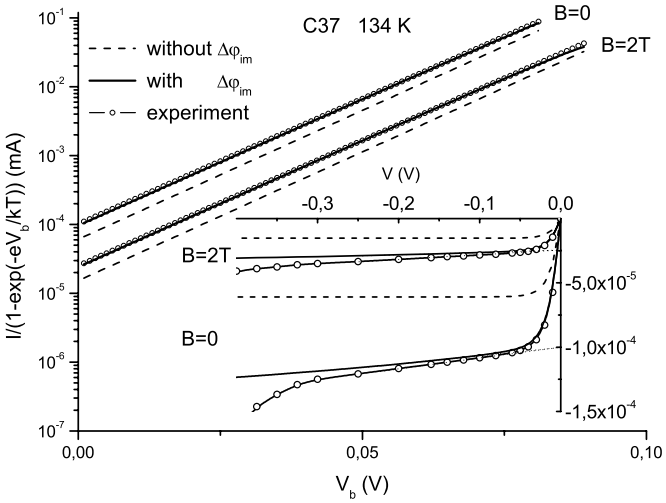

Figure 3. The forward and reverse (insert) voltage–current characteristics with and without allowance for the barrier height lowering due to the image force.

decrease in the saturation current I_s (the intercept points with ordinate axis in figure 2).

At the same time, as can be seen in figure 2, the reverse current slowly increases (near-linearly at low biases) with the applied voltage. Nevertheless, even if a reverse current does not saturate, the value of I corresponding to the interception at the ordinate of the linear segment of the reverse branch of the experimental I–V characteristic is in close agreement with the saturation current determined from a forward branch. The bias dependence of a reverse current can be satisfactory explained if the barrier height lowering due to the image force is taken into account [9]

$$\Delta\varphi_{\rm im} = \left[\frac{e^2(N_A - N_D)}{8\pi^2(\varepsilon\varepsilon_0)^3}\,(\varphi_B - \eta - eV - kT)\right]^{1/4}. \qquad (7)$$

In contrast to 'classical' semiconductors, the energy gap E_g and consequently the barrier height φ_B in narrow-gap $Hg_{1-x}Cd_xTe$ (at $x < 0.5$) increases with temperature [10]

$$E_g(x,T) = -0.302 + 1.93x - 0.810x^2 + 0.832x^3 + 5.35\cdot 10^{-4}(1-2x) \times [(T^3 - 1822)/(T^2 + 255.2)] \qquad (8)$$

(for E_g expressed in eV and T in K). Assuming that the barrier height varies with temperature the same way as does the band gap and that the Fermi level at the interface is fixed at the energy being a fixed fraction of the energy gap, the temperature dependence of φ_B can be described as

$$\varphi_B(T) = \varphi_B(0) + \gamma\alpha kT, \qquad (9)$$

where the temperature coefficient of the energy gap γ can be calculated from expression (8) as $\gamma = {\rm d}E_g/{\rm d}kT \approx 6.21(1-2x)$ and α is the ratio φ_0/E_g at zero temperature (see table 1). The increase of the potential barrier height with temperature is clearly evident in the anomalous temperature dependence of the reverse tunnelling current, which dominates at $T < T_0$. The interband and trap-assisted tunnelling currents decrease by a factor 10 or more in the temperature range of 20 K $\leqslant T \leqslant$ 80 K. The dependence (9) describes very well the magnetic field dependences of the tunnelling current investigated in similar Pb-p-HgCdTe SB in [4]. The $\Delta\varphi_{\rm im}$ values calculated for zero bias and $T = 140$ K are presented in table 1. The Fermi energies η were calculated from the neutrality equation taking into account the non-parabolicity in a three-band Kane approximation.

The I–V characteristics calculated with allowance for the image force

$$I = I_0 \exp\left[\frac{\Delta\varphi_{\rm im}(V)}{kT}\right]\left[\exp\left(\frac{eV}{kT}\right) - 1\right] = I_s(V)\left[\exp\left(\frac{eV}{kT}\right) - 1\right] \qquad (10)$$

are compared with those measured experimentally in figure 3 for the same sample, temperature and magnetic fields as shown in figure 2. It is seen that at low biases the calculated reverse current indeed shows linear bias dependence. For calculations, the input saturation current I_0 was chosen so that the intercepts at the ordinate of the linear portions of the calculated current (calculated with allowance for the image force) were equal to the experimental reverse characteristics I_s. Simultaneously, the same accordance occurs for forward branches as well (see figure 3). The barrier height lowering causes a 4–6 % increase in the slope of the forward $\ln I$–V characteristic in accordance with the experimental value of the ideality factor $\beta = 1.04$–1.05. The modified (by barrier lowering) saturation current I_s is higher by a factor of ≈ 1.6 than the input saturation current I_0. The I_s/I_0 ratio decreases only slightly with an increasing temperature. For the temperature range investigated, the I_s/I_0 ratio ranges from 1.6 to 1.3 for PK2 and C37 samples and from 2 to 1.6 for strongly doped sample C36. The near-constant slope of the reverse characteristics at low biases can formally be considered as an effective leakage conductance. Its value has a temperature dependence close to the one for the saturation current that agrees satisfactorily with the experiment. Because the function $\exp(\Delta\varphi_{\rm im}/kT)$ in expression (10) appears as a magnetic field-independent

multiplier, I_s varies with magnetic field exactly as does I_0 (figure 3).

While the barrier height increases with the temperature, the diffusion potential φ_{d0} falls because of the increasing Fermi energy η. On the other hand, the saturation current exponentially increases with the temperature. This leads to an increase in the voltage drop across a series resistance in spite of the fact that the resistance decreases with T at high temperatures. Note that the contribution of the voltage drop across the series resistance to the I–V experimental plot can be reduced by an order of magnitude if a three-terminal method of measurement is applied. In this case, the ohmic contacts on the opposite sides of substrate wafer are used as current contact and potential probes, respectively. The higher the diffusion potential and lower the series resistance, the greater the range over which the $\ln I$–V curve follows a straight line. As the range of the exponential dependence of the forward I–V plots shrinks with temperature, the accuracy of the determination of the saturation current and β from the forward branch at high temperatures becomes poor. In this case, the relation $\ln((I - VG_l)/I_s + 1) = e(V - IR_s)/\beta kT$ was fitted to the data in the bias range of $-2kT < eV_b < \varphi_{d0}$ using I_s and β as adjustable parameters. The values of R_s and the effective leakage conductance G_l were determined from forward and reverse I–V characteristics in sufficiently high-bias regions. The I_s values obtained in such a way are in reasonable agreement with those determined from the reverse branches of I–V characteristics.

4. Magnetic field dependence of the saturation current

To find out the character of $I_s(B)$ dependences, the currents at fixed forward and (or, at high temperatures) reverse biases were recorded as a function of the magnetic field. The biases were chosen so that they corresponded to the beginning of linear segments of I–V and $\ln I$–V characteristics for reverse and forward biases, respectively. In the first case, the correction for the change in the slope of an I–V plot in a magnetic field was taken into account using the records of I–V characteristics at 4–6 fixed values of magnetic field (similarly to the figure 2). Typical magnetic field dependences of the normalized saturation current $I_s(B)/I_s(0)$ for the same sample as in figure 2 are shown in figure 4. The magnitude of the effect decreases with increasing temperature (figure 4(b)) and composition x (figure 4(a)). This is particularly evident in the range of relatively small magnetic field, $B < 1$ T. At higher magnetic field, the $I_s(B)/I_s(0)$ dependences exhibit a tendency toward saturation but do not reach overall saturation in the range of magnetic fields investigated. At highest available magnetic field, $B = 5$ T, the $I_s(B)/I_s(0)$ values vary from diode to diode even within the series of one sample type. At low temperature at $T \sim 120$ K, the ratio $I_s(B_{\max})/I_s(0)$ varies from 0.04 to 0.15 and increases with temperature.

If the over-the-barrier transport is due to heavy holes, as it is customarily supposed, we are to expect a pronounced effect only at extremely strong magnetic fields within the framework of both diodes ($B > 20$T) and diffusion ($B > 10$ T) theory.

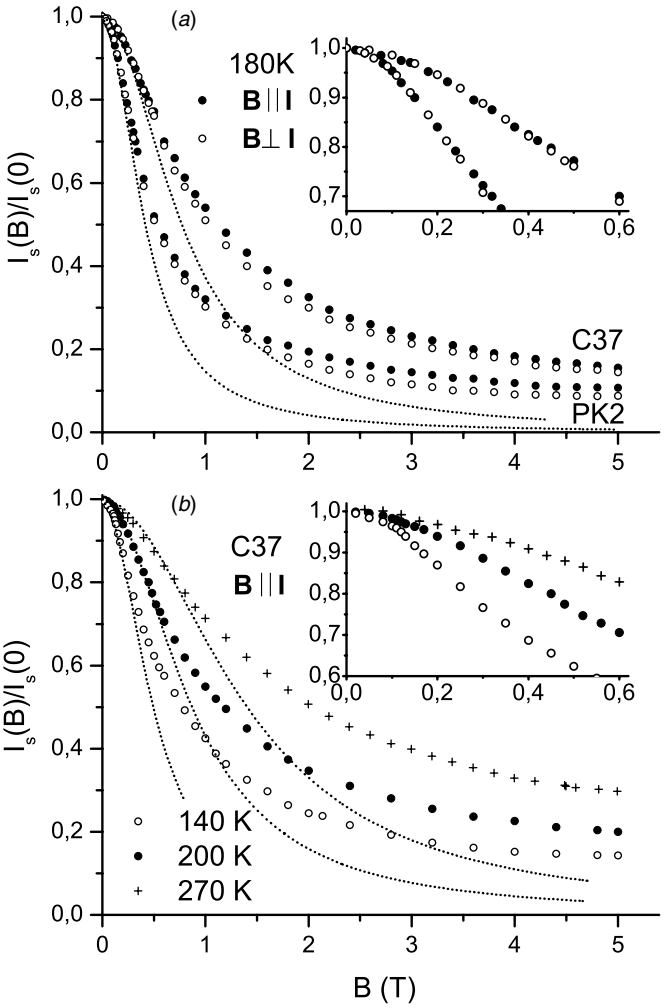

Figure 4. Typical magnetic field dependences of the normalized saturation current for samples with different light hole effective masses at various temperatures. The dotted lines were calculated using relation (11).

However, experimentally more than a twofold decrease in I_s is observed, even at $B < 0.5$ T for sample with $x = 0.22$ and $B < 1$ T for samples with $x = 0.29$. These small values of B correspond to $\theta \sim 1$ and $\mu B \sim 1$, that is for carriers with light mass, and therefore we can assume that the heavy holes do not contribute significantly to the over-the-barrier current. This is in agreement with the fact that the magnitudes of B corresponding to the same value of $I_s(B)/I_s(0)$ are approximately twice as large for material with $x = 0.29$ than for sample with $x = 0.22$ (compare curves in figure 4(a)) in accordance with the ratio of light carriers masses and mobilities, whereas the effective mass and mobility of heavy holes for both compositions are the same. The contribution of heavy holes to the total current is manifested by the saturation region of $I_s(B)$ dependences at high magnetic fields.

First, we analyse $I_s(B)$ dependences at low magnetic fields, where the ratio $I_s(B)/I_s(0) > 0.7$. In this case as a first approximation, one can neglect the contribution of heavy

holes. In figure 4, we plot the $I_s(B)/I_s(0)$ *versus* B data and compared with the appropriate calculated results

$$I_s(B)/I_s(0) = 1/(1 + (\mu_{lh}(0)B)^2), \tag{11}$$

which are expected for the effect caused by the suppression of the carrier mobility in a magnetic field. The light hole mobility in a zero magnetic field, $\mu_{lh}(0)$ in relation (11), was evaluated according to the empirical expression for electron mobility in n-type HgCdTe [2]

$$\mu_e = 9 \times 10^8 \frac{b^{7.5}}{T^{2b^{0.6}}} \tag{12}$$

where $b = 0.2/x$ and T and μ are expressed in Kelvin and $cm^2\ V^{-1}\ s^{-1}$, respectively. In the low-magnetic field range, figure 4 shows a good fit between the relation (11) and the data. However, it should be noted that the light hole mobility in p-type HgCdTe can differ from the values given by expression (12) [11, 12]. For heavy holes, the magnitude of the effect expected at $B = 5$ T does not exceed 0.3 % even at lowest temperatures. As the light hole mobility (12) decreases with the temperature and composition x, the magnitude of the effect should also decrease. This is in agreement with the data presented for samples with different composition in figure 4(*a*) and at various temperatures in figure 4(*b*).

At a first sight, the magnetic field dependence of the saturation current can be qualitatively explained (at low magnetic fields, quantitatively) by the suppression of the carrier mobility. However, this is not the case. The point is that the magnitude of the effect described by equation (11) is determined by a magnetic field component which is perpendicular to the current flow direction and the effect should be absent in the **B** ∥ **I** orientation. However, the measurements in tilted magnetic fields show that the magnitude of the effect, $I_s(B)/I_s(0)$, only weakly depends on the angle between **B** and **I**. It is seen in figure 4 that the magnetic field effect at **B** ⊥ **I** is somewhat larger than at **B** ∥ **I**, but the difference is small. For low magnetic fields at which $I_s(B)/I_s(0) > 0.7$, the magnitude of the effect is practically the same in both orientations (see the inset in figure 4(*a*)). In the **B** ∥ **I** orientation, the magnetic field effect on the saturation current can be caused only by the increase of the barrier height with **B** because of the magnetic quantization of the light hole spectrum.

Because the magnitude of the magnetic field effect does not depend on the mutual orientation of **B** and **I**, one can conclude that the suppression of the mobility does not contribute to the $I_s(B)$ dependence either at **B** ∥ **I** or at **B** ⊥ **I** (or any tilted) orientation. On the other hand, the magnetic field dependence of the mobility can result in the suppression of the saturation current only in the case of a diffusion limited over-the-barrier current (see equation (2*b*)). In the case of thermionic emission, the carriers move ballistically in the space-charge region of Schottky barriers and the current does not depend on the mobility (the expression for thermionic current, (2*a*), does not contain the mobility). These observations allow one to conclude that the diffusion current does not contribute significantly to the total current in the SB studied and that the thermionic emission of light holes is the dominant carrier transport mechanism. Thus, one can see that the use of magnetic field enables not only the experimental separation of light and heavy carriers, but also between different carrier transport mechanisms (using tilted magnetic fields). The above conclusion regarding the dominance of the light hole thermionic emission is in good agreement with the fact that the $\mu_{lh}E_m/\overline{v}_{lh}$ ratio, usually used as a criteria for the identification of a dominant carrier transport mechanisms in SB, varies within the limits of 25–2.5 in the temperature range of 100–250 K for the investigated samples. Very similar values are obtained for Bete's ratio $2\varphi_0 kT/\ell W \sim 25$–3; here, ℓ is a mean free path and W is the width of the space-charge region. This also provides convincing evidence that the dominant carrier transport mechanism for light holes, at least at $T < 230$–250 K, is thermionic emission. For heavy holes in the same temperature range, this ratio $\mu_{hh}E_m/\overline{v}_{hh} \approx 0.7$–0.2 is significantly lower, so that in the case of heavy-hole transport over-the-barrier the contribution of the diffusion component can be significant.

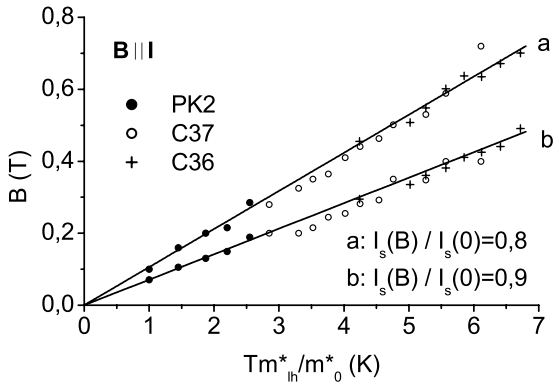

Figure 5. Experimental dependence of the magnetic field corresponding to a given ratio $I_s(B)/I_s(0)$ versus the product of temperature and light hole effective mass (taking into account its temperature dependence).

As was previously mentioned, there is a strict correlation between the magnitude of the effect and the effective mass of light carriers. Analysis of the data for different alloy composition x and temperatures $T \geqslant T_0$ (m^*_{lh} changes not only with x, but also with T) shows that the values of B corresponding to the same magnitude of the effect at $I_s(B)/I_s(0) > 0.7$ are proportional to the product Tm^*_{lh}. This is clearly seen in figure 5. From this, the conclusion follows that a value of the magnetic field effect, at least at low magnetic fields when $I_s(B)/I_s(0) > 0.7$, is indeed uniquely determined by the ratio B/Tm^*_{lh} or, in energy units, by the parameter $\theta = \hbar\omega_{clh}/kT$.

At higher magnetic fields, the $I_s(B)$ dependences can be affected by the contribution of heavy holes. As mentioned above, the relative contribution of heavy holes in different SB studied may be different because of the uncontrolled scatter of the oxide layer parameters (mainly the layer thickness), and, in principle, can be temperature dependent because of the temperature dependence of the light hole effective mass. To compare $I_s(B)$ dependences for different samples and temperatures and to clarify the character of $I_s(\theta)$ dependences in high magnetic field, the normalized saturation current fractions $(I_s(B) - I_{s0})/(I_s(0) - I_{s0})$ controlled by the light carriers were plotted as a function of the parameter θ (see

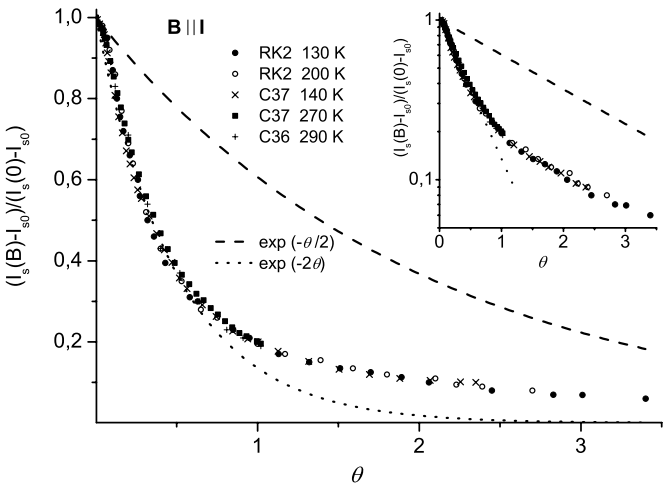

Figure 6. The values of $(I_s(B) - I_{s0})/(I_s(0) - I_{s0})$ fraction obtained on three different samples at various temperatures are plotted *versus* θ. The curves are matched at a point $\theta = 1$ using I_{s0} as an adjusting parameter. The broken and dotted lines show calculation results involving equation (13) with n = 1/2 and n = 2, respectively.

figure 6). Here I_{s0} is a possible residual contribution of heavy holes (unaffected by the magnetic field at $B < 5$T) to the total saturation current. The matching parameters I_{s0} for each sample and the temperature were determined experimentally from the condition that $(I_s(B) - I_{s0})/(I_s(0) - I_{s0}) = 0.2$ at $\theta = 1$. This relation used for matching corresponds to the SB with the smallest saturation current at $B = 5$ T. In accordance with a difference in the values of the effect at maximum magnetic field $B \simeq 5$T, magnitudes of the fraction I_{s0} vary from sample to sample. As a rule, the values of I_{s0} are larger for wider gap samples such as C36 and C37 (with $J_{s0}/J_s(0) \sim 0.06 \div 0.15$) than for narrower gap sample PK2 (with $I_{s0}/I_s(0) \sim 0.015 \div 0.08$). I_{s0} is also larger in a crossed orientation as compared to the case where $\mathbf{B} \parallel \mathbf{J}$. In spite of an uncontrolled scatter in the parameters of the oxide layer, the dependence of the fraction $I_s(B) - I_{s0}$ on the parameter θ fits a common universal curve for all samples, temperatures and orientations of B (see figure 6). Thus, it is possible to assume that the magnitude of the magnetic field effect is determined by the ratio $\hbar\omega_c/kT$ for light holes for not only small B, but over the whole range of magnetic fields used here. This result, along with the absence of B orientation dependence, supports the conclusion that the magnetic field effect for thermionic emission is due to magnetic quantization of the light hole spectrum.

Within the framework of this interpretation the effective Kane's gap for light carriers (the gap between light hole and electron bands) increases with the magnetic field because of Landau quantization. Because the condition $\hbar\omega_c \ll E_g$ is satisfied in the range of magnetic fields used, one can neglect the non-parabolicity effects. In this case, $\Delta E_g(B)$ is given by $\Delta E_g(B) = \hbar\omega_c = \hbar eB/m^*_{\rm lh}$ (we also neglect spin effects). On the other hand, because of the high density of states in the heavy-hole band, the bulk Fermi energy η and barrier width are determined by the heavy-hole majority carriers (while the current is controlled mainly by light holes, due to a blocking of heavy-hole flow by the insulating layer). Because the heavy-hole band is unaffected by the magnetic field, one can assume that the Schottky barrier height for light holes φ_B increases by $\Delta\varphi_B = n\hbar\omega_c$, where $n = 1/2$ without taking into account the spin splitting. Within this model, the dependence of I_s on B according to equation (2*a*) is expected to be

$$\frac{I_s(B) - I_{s0}}{I_s(0) - I_{s0}} \approx \frac{I_{s\rm lh}(B)}{I_{s\rm lh}(0)} = \exp -n\theta. \qquad (13)$$

However, the experimental magnetic field dependence of the saturation current is more complicated and quantitatively does not follow this model. The magnitude of the magnetic field effect exceeds considerably the prediction of the simple theory (13) (the fit by expression (13) with $n = 1/2$ is shown by a dashed line in figure 6). For small $\theta < 0.5$, the ratio $(I_s(B) - I_{s0})/(I_s(0) - I_{s0})$ dependence on θ can be roughly described by equation (13), only if the factor $n = 2$ is chosen (dotted line in figure 6). The reasons of this discrepancy are not understood. It is clear, that accounting for non-parabolicity and Zeeman splitting should only reduce the magnitude of the expected effect.

In spite of the noted quantitative discrepancy, we argue that the over-the-barrier carrier transport in Schottky barriers is controlled by the thermionic current of light carriers. In order to corroborate that further, the temperature dependence of the saturation current, which is usually used to determine the Richardson constant, was re-analysed in the next section. Similar temperature dependences were discussed earlier in [3, 13, 14].

5. Richardson plot

The effective Richardson constant for heavy holes in $Hg_{1-x}Cd_xTe$ is expected to be $A^*_{\rm hh} \approx 6 \times 10^5$ A m^{-2} K^{-2}. For light holes, $A^*_{\rm lh}$ is not only composition but also temperature dependent, because of the temperature dependence of the light hole effective mass $m^*_{\rm lh}(T)/m^*_{\rm lh}(0) = E_g(T)/E_g(0)$. For sample PK2 (C37) in the investigated temperature range $m_{\rm lh}$ increases almost by 80 % (by 30 %) as compared to its value at T = 0. For this reason, the standard relationship (2*a*) used to determine the Richardson constant has to be corrected as follows:

$$\ln \frac{I_s}{ST^2[1 + \gamma kT/E_g(0)]} = \ln A^*_{\rm lh0} - \frac{\varphi_0}{kT}, \qquad (14)$$

where $A^*_{\rm lh0}$ is the Richardson constant corresponding to the light hole effective mass at zero temperature. The Richardson curves plotted in this way are shown in figure 7. The term in square brackets in expression (14) notably reduces the slope of the Richardson plot but does not affect the intercept at the ordinate. Neglecting the temperature dependences of the effective mass results in an overestimation of the barrier height by ~3–5%.

As seen in figure 7(*b*), the data follow the linear dependence on $1/T$ and equation (14) retains its validity up to temperatures of $T \sim 140$ K for sample with $x = 0.221$ and $T \sim 180$K for samples with $x = 0.29$. At higher temperatures, an increase in the slope is observed. The value of 150 (60) A m^{-2} K^{-2} for sample PK2 (C37) is determined from an extrapolated intercept of the experimental Richardson plot

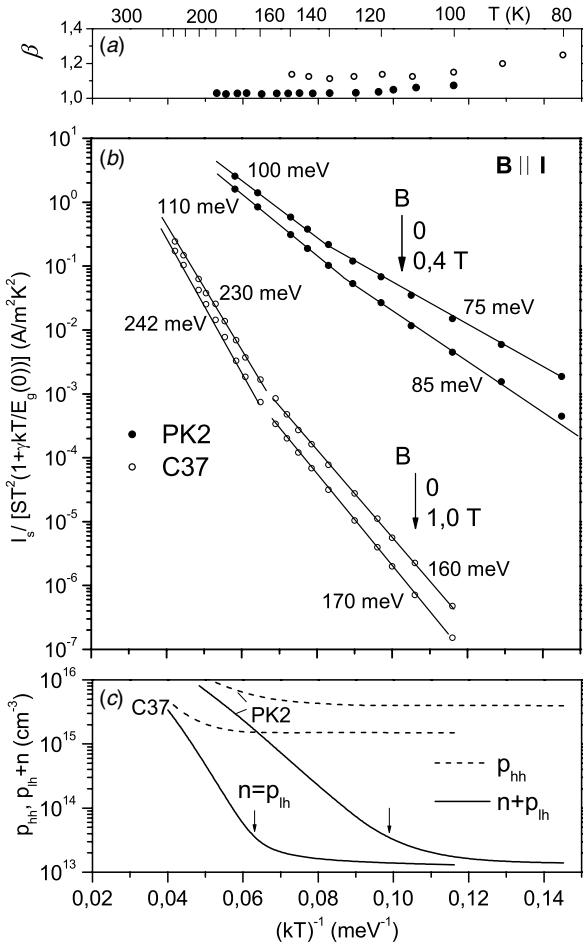

Figure 7. Temperature dependences of the ideality factor (*a*) saturation current (*b*) and carrier concentrations in the quasineutral p region of SB (*c*). The numbers at the linear segments of plots in figure 7(*b*) are the slope values.

(14) in its low-temperature linear segment. These apparent magnitudes of the Richardson constant are much lower than their theoretical values, not only for heavy holes (by a factor of $\sim 5 \times 10^3$) but also for light holes (by a factor of $\sim 10^2$). However, there are two factors which should change the intercept of the experimental Richardson plot in comparison with A^*_{lh0}: the temperature dependence of the barrier height and tunnelling penetration through the insulator layer. When the temperature dependence of the barrier height (9) and the penetration coefficient (4) of the interfacial insulator layer for light holes P_{lh} are taken into account, the relationship (14) is modified as

$$\ln \frac{I_s}{ST^2[1+\gamma kT/E_g(0)]} = \ln P_{\mathrm{lh}} A^*_{\mathrm{lh0}} - \frac{\varphi_0(0)+\alpha\gamma kT}{kT}. \quad (15)$$

At linear temperature dependence of the energy gap E_g (γ = const), the dependence $\ln I_s/[1ST^2[1+\gamma kT/E_g(0)]]-T^{-1}$ is linear, with the slope determined by the barrier height $\varphi_0(0)$ at $T = 0$. It is seen from expression (15) that allowing for temperature dependence of the barrier height leads to a change in a value of the intercept at the ordinate of the Richardson plot. Because $\gamma > 0$ in samples under the investigation, the apparent effective Richardson constant decreases. This is opposite to the effect predicted for SB on the base of 'classical' semiconductors, where the Richardson constant is modified to higher values because of the negative temperature coefficient of the band gap and barrier height [15, 16].

It is clear that the introduction of the penetration coefficient P_{lh} is practically equivalent to the reduction of the Richardson constant. Unfortunately, at present we have no correct theoretical description of the $I_s(B)$ dependence for the light holes. If such dependence was known, it would be possible to determine the contribution of heavy holes to the total current by fitting the calculated $I_{s\mathrm{lh}}(B) + I_{s\mathrm{hh}}$ dependence to the experimental one. Using the ratio $I_{s\mathrm{hh}}/I_{s\mathrm{lh}}$ obtained this way, one can find the parameter $\delta\sqrt{\varphi_{\mathrm{ox}}}$ from equation (5) and therefore determine P_{lh}. As a first-order estimation for $I_{s\mathrm{hh}}$ (upper bound), the values of the saturation current at a highest available magnetic field B_m and at lowest temperature may be used. The ratio $I_s(B_m)/I_s(0)$ ranges from 0.04 to 0.1. Using these values, the quantity $\delta\sqrt{\varphi_{\mathrm{ox}}}$ can be estimated from equation (5) as (0.95–1.1) nm $\mathrm{eV}^{1/2}$, which gives $P_{\mathrm{lh}} \sim (0.3-0.35)$ for $x = 0.221$ and $P_{\mathrm{lh}} \sim (0.2-0.25)$ for $x = 0.29$ (for heavy holes $P_{\mathrm{hh}} \sim (4-10)\times 10^{-4}$). It should be noted that though the separative role of the oxide layer must be more pronounced in narrow-gap semiconductors, the ratio (5) weakly depends on the composition x and temperature. It ranges from 0.075 to 0.06 in the composition interval of $x = 0.17$–0.4 and temperature range of $T = 100$–250 K if $\delta = 1$ nm assuming $\varphi_{\mathrm{ox}} = 1$ eV (even in SB on p-Si $I_{s\mathrm{hh}}/I_{s\mathrm{lh}} \approx 0.15$ at the same δ and φ_{ox}). On the other hand, the $I_{s\mathrm{hh}}/I_{s\mathrm{lh}}$ ratio strongly depends on the height and thickness of the barrier. For the same $\delta = 1$ nm, but for $\varphi_{\mathrm{ox}} = 1,5$ eV the equation (5) gives $I_{s\mathrm{hh}}/I_{s\mathrm{lh}} = 0.019$–$0.017$ in the same temperature and composition ranges.

As may be inferred from expression (15) the true Richardson constant A^*_{lh0} and apparent effective Richardson constant A^{**}_{lh0} (experimentally determined from the Richardson plot as the intercept at the ordinate) are related by the expression

$$A^*_{\mathrm{lh0}} = \exp(\alpha\gamma/k) P_{\mathrm{lh}}^{-1} A^{**}_{\mathrm{lh0}}. \quad (16)$$

The Richardson constant A^*_{lh0} estimated from this relation for sample PK2 is 8.2×10^3 A m^{-2} K^{-2}, taking into account the above determined values of A^{**}_{lh0} and P_{lh}. This is in close agreement with the theoretically expected value of 8.8×10^3 A m^{-2} K^{-2}. Similar estimations for samples C37 and C36 give $A^*_{\mathrm{lh0}} \sim (2.2$–$2.5)\times 10^3$ A m^{-2} K^{-2} for both samples and this is less than the expected value of 2×10^4 A m^{-2} K^{-2}.

In figure 7 the Richardson curves, measured in low magnetic fields where the heavy holes do not contribute significantly to the total current, are also plotted. No peculiarities are observed in the Richardson plot in a magnetic field as compared to the $B = 0$ case. The effect of the magnetic field is seen only as an increase in the slope of Richardson plots that indicates a rise in the Schottky barrier height. The apparent effective Richardson constant A^{**}_{lh0} is practically unaffected by the magnetic field. The slope of the Richardson plot increases by $\Delta\varphi_b \sim (10$–$12)$ meV in the range of magnetic fields used. These values are approximately 3–4 times higher than those expected for light holes, due to the increase in the barrier height $\Delta\varphi_B = \hbar\omega_c/2$ ($\Delta\varphi_B \approx 2.3$ meV for $x = 0.221$

and $\Delta\varphi_B \approx 3$ meV for $x = 0.29$). Thus, there is the same inconsistency, which was already emphasized in section 4, when discussing effects of the magnetic field on the saturation current. Namely, equation (13) accounted for the data if n = 2 was used instead of n = 1/2.

As mentioned, the $I_s(T)$ dependence cannot be accounted for by equation (15) at all the temperatures we used. The Richardson plot is in fact composed of the two linear regions (figure 7(*b*)). The previous analysis in this section was concerned with a low-temperature segment of the Richardson plot. At higher temperatures, the slope for both samples increases to the value close to E_g. The intercept at the ordinate in this region for sample PK2 (C37 and C36) is an order (two orders) of magnitude higher than its value in the low-temperature portion. These values are an order of magnitude higher than the theoretically expected values of the Richardson constant, A^*_{lh0}, for light carriers.

A possible reason for the 'two-region' behaviour of the $\ln I_s(T)$ dependences is the contribution of the minority carriers (electrons) to the total current at high temperatures. Because heavy holes are removed from the transport by the interface oxide layer, the contribution of the electrons may be significant even at moderate temperatures at which the transition to intrinsic conductivity is only beginning. In figure 7(*c*), the temperature dependences of p_{hh} and $p_{\mathrm{lh}} + n_e$ concentrations calculated from the electroneutrality equation are plotted. The band non-parabolicity for light carriers and temperature dependences of Kane's band gap E_g and effective masses m^*_{lh} and m^*_e were taken into account. It is seen that a notable increase in p_{hh} concentration starts at $T \sim 180$ K for $x = 0.22$ and at $T \sim 220$ K for $x = 0.29$, whereas the contribution of electrons to the total concentration of light carriers is essential already at $T \sim 120$ K for $x = 0.22$ and $T \sim 160$ K for $x = 0.29$ (the temperatures at which $n_e = p_{\mathrm{lh}}$ are marked by the arrow in figure 7(*c*)). Exactly above these temperatures the change in the slope of Richardson plots is observed. The activation energy of the $p_{\mathrm{lh}} + n_e$ concentration for this transition temperature region of T is close to E_g (at higher T this energy approaches $E_g/2$) which is close to the slope of the high-temperature region of the Richardson plot. Figure 7(*b*) shows that in a magnetic field, the increase in the slope of the Richardson plot in its high-temperature segment is practically the same as in the low-temperature range (within experimental error) which in turn is in good agreement with the equality of the cyclotron energies of light holes and electrons.

6. Summary and conclusion

A strong magnetic field effect on the over-the-barrier transport in Schottky barriers on p-type narrow-gap $Hg_{1-x}Cd_xTe$ is revealed and is investigated in a wide temperature interval. The large magnitude of the effect indicates that the over-the-barrier current is carried by light holes. The weak dependence of the effect value on the magnetic field orientation manifests that this effect cannot be attributed to the suppression of light hole mobility by the magnetic field (this suppression should vanish in **B** ∥ **I** orientation) and thus the over-the-barrier transport is mainly due to the thermionic emission (ballistic carrier transport) but not a diffusion current (mobility controlled transport). The predominance of light holes in the carrier transport in SB fabricated on p-type semiconductor should be expected because of the low tunnelling penetrability of heavy holes through the interface oxide layer inevitably existing in real Schottky diodes. This assumption, in conjunction with the temperature dependence of the barrier height, satisfactorily explains the experimental values of the Richardson constant.

Our study, carried out on materials with several different band parameters and at varying temperatures, indicates that the magnitude of the magnetic field effect is uniquely determined by the ratio of the light hole cyclotron energy to the thermal energy $\theta = \hbar\omega_{c\mathrm{lh}}/kT$. However, the magnitude of the effect exceeds considerably the prediction of a simple theory, and the experimental dependences of the saturation current do not follow a simple exponential decay ($\propto \exp(-\theta/2)$) predicted for the thermionic current. Thus, a more sophisticated theoretical model is needed for accounting for the data. It would be interesting to investigate the magnetic field effect in similar SB grown on the n-type narrow gap $Hg_{1-x}Cd_xTe$. Unfortunately, as was mentioned earlier, such barriers do not exhibit rectifying properties. Another possible subject of inquiry is the magnetic field effects on the carrier transport in $Hg_{1-x}Cd_xTe$ p−n junctions. The first preliminary results of such research we performed reveal a strong effect at both orientations of the magnetic field. The magnetic-field dependences of the saturation current in the p−n junction are in general similar to those in SB, but there are some specific features that need special consideration far beyond the scope of this paper.

As the oxide layer blocks the heavy-hole tunnelling, the light holes are responsible for carrier transport in SB on p−type HgCdTe in both regimes of tunnelling at low temperatures $T < T_0$ and over-the-barrier transport at $T > T_0$. It should be noted that the effect of the insulator layer on the thermionic current discussed here does not affect the results in [3, 4], which investigate tunnelling and magneto-tunnelling in SB on p−HgCdTe at low temperatures $T < T_0$. The influence of this layer on the tunnelling current is negligible, because its tunnelling transparency for light holes $P_{\mathrm{lh}} \sim 0.2$–0.4 exceeds by many orders of magnitude the transparency of the depletion layer $P_{\mathrm{SB}} \sim \exp(-\lambda_0)$ where $\lambda_0 = 5$–30 [4].

The experimental results discussed here show that the prevalence of light holes in the over-the-barrier current should be taken into account in the analysis of the carrier transport in Schottky barriers fabricated on p-type semiconductors, especially in metal–insulator–semiconductor Schottky diodes [6, 7, 17].

References

[1] Rogalsky A 2003 *Prog. Quantum Electron.* **27** 59
[2] Rogalsky A 2005 *Rep. Prog. Phys.* **68** 2267
[3] Zavyalov V V, Radantsev V F and Deryabina T I 1992 *Fiz. Tekh. Poluprov.* **26** 691
Zavyalov V V, Radantsev V F and Deryabina T I 1992 *Sov. Phys.—Semicond.* **26** 388 (Engl. transl.)
[4] Zavyalov V V and Radantsev V F 1994 *Semicond. Sci. Technol.* **9** 281

[5] Sze S and Ng K 2008 *Physics of Semiconductor Devices* 3rd edn (New York: Wiley)
[6] Yildiz D E, Altindal S and Kanbur H 2008 *J. Appl. Phys.* **103** 124502
[7] Damnjanovic V, Ponomarenko V P and Elazar Jovan M 2007 *Semicond. Sci. Technol.* **22** 137
[8] Williams G M and DeWames R E 1995 *J. Electron. Mater.* **24** 1239
[9] Rhoderick E H and Williams R H 1988 *Metal Semiconductor Contacts* 2nd edn (Oxford: Claredon)
[10] Seller D G and Lowney J R 1990 *J. Vac. Sci. Technol.* A **8** 1237
[11] Schacham S E and Finkman E 1986 *J. Appl. Phys.* **60** 2860
[12] Gold M C and Nelson D A 1986 *J. Vac. Sci. Technol.* A **4** 2040
[13] Polla D L and Sood A K 1980 *J. Appl. Phys.* **51** 4908
[14] Bahir G, Adar R and Fastov R 1991 *J. Vac. Sci. Technol.* B **9** 266
[15] Missous M and Rhoderick E H 1991 *J. Appl. Phys.* **69** 7142
[16] Missous M, Rhoderick E H, Woolf D A and Wilkes S P 1992 *Semicond. Sci. Technol.* **7** 218
[17] Mikhelashvili V, Eisenstein G, Garber V, Fainleib F, Bahir G, Ritter D, Orenstein M and Peer A 1999 *J. Appl. Phys.* **85** 6873